Multiscale Penalized Weighted Least-Squares Sinogram Restoration for Low-Dose X-Ray Computed Tomography

Jing Wang, Zhengrong Liang, *Senior Member, IEEE*, and Hongbing Lu, *Member, IEEE*

Abstract—We propose a novel multiscale penalized weighted least-squares (PWLS) method for restoration of low-dose computed tomography (CT) sinogram. The method utilizes wavelet transform for the multiscale or multi-resolution analysis on the sinogram. Specifically the Mallat-Zhong's wavelet transform is applied to decompose the sinogram to different resolution levels. At each decomposed resolution level, a PWLS criterion is applied to restore the noise-contaminated wavelet coefficients, where the penalty is adaptive to each resolution scale and the weight is adaptive to each scale and each location. The proposed PWLS method is based on the observation that (1) the noisy sinogram of low-dose CT after logarithm transform can be modeled as signal-dependent Gaussian variables and the sample variance depends on the sample mean; and (2) the noise restoration can be more effective when it is adaptive to different resolution levels. The effectiveness of the proposed multiscale PWLS method is validated by an experimental study. The gain by multiscale approach over single-scale means is quantified by noise-resolution tradeoff measures.

I. INTRODUCTION

Low-dose computed tomography (CT) is clinically desirable, especially for screening purpose. A simple and cost-effective means among many other approaches to achieve low-dose CT is to lower the X-ray tube current (mA) or deliver less X-rays. However the image quality with low mA acquisition protocol could be severely degraded due to the excessive X-ray quantum noise [1-3]. Many strategies have been proposed to reduce the noise, *e.g.*, by nonlinear noise filters [1-3] and statistics-based iterative image reconstructions (SIIRs) [4-5]. The nonlinear filters do not explicitly consider the statistical distribution of the noise and the SIIRs are notorious for their excessive computational demands for large CT data size. Recently, statistics-based sinogram smoothing approaches [6-7] followed by filtered back-projection (FBP) image reconstruction have shown the potential for noise reduction and edge-preservation in low-dose CT imaging. These statistics-based sinogram smoothing approaches fully utilized the statistical

information of measured data while avoid the time consuming projection-backprojection cycles in the SIIRs. So far these sinogram-smoothing approaches have been implemented in a single-scale sinogram space.

Wavelet theory on multiscale image analysis has been extensively studied and widely applied in image restoration [8-10]. Most of the previously developed wavelet-based de-noising algorithms either assume a Gaussian white noise for the data or estimate the local statistics of the image (*e.g.*, the variance of a pixel from its neighbor). The Gaussian white noise assumption is not valid for the CT sinogram, because the detected counts follow a Compound Poisson distribution and the noise in the log-transformed sinogram follows a signal-dependent Gaussian distribution [3, 6]. Estimation of variance from local statistics may lead to inaccuracy [6].

In this paper, we propose a novel multiscale penalized weighted least-squares (PWLS) method for restoration of low-dose CT sinogram. The Mallat-Zhong's wavelet transform [11] is first applied to decompose the sinogram image to different resolution scales. In the wavelet domain, noise is dominant in those wavelet coefficients at the lower decomposition levels [11]. Based on this observation, a PWLS criterion is applied adaptively to restore the wavelet coefficients. The multiscale PWLS method fully utilizes the statistical information of the sinogram data [3, 6] and also considers the characteristics of the signals from multiscale decomposition of the image data [11].

II. METHOD

A. Mallat-Zhong's Dyadic Wavelet Transform

In [11], Mallat and Zhong presented a dyadic wavelet transform (DWT) and developed a fast algorithm to compute the DWT, which involves the convolution of the image $f(x,y)$ with a set of low-pass filter H and high-pass filters G and D:

$$W_{2^{j+1}}^1 f(x,y) = S_{2^j} f(x,y) * (G_j, D) \tag{1}$$

$$W_{2^{j+1}}^2 f(x,y) = S_{2^j} f(x,y) * (D, G_j) \tag{2}$$

$$S_{2^{j+1}} f(x,y) = S_{2^j} f(x,y) * (H_j, H_j) \tag{3}$$

where D is the Dirac filter and G_j and H_j denote their corresponding discrete filters obtained by putting 2^j -1 zeros between consecutive coefficients of their defined filter G or H [11]. Operation $A*(D,G_j)$ denotes the separable convolution of the rows and columns of an image A with the 1D filters D and G. $S_{2^j} f(x,y)$ denotes the approximation of $f(x,y)$ at scale 2^j and $\{(W_{2^j}^1 f(x,y))_{1\le j\le J}, (W_{2^j}^2 f(x,y))_{1\le j\le J}\}$ represents the detail image at scale 2^j. The inverse wavelet transform can be obtained by the following recursive

formula:

$$S_{2^{j-1}}f(x,y) = W^1_{2^j}f(x,y)*(K_{j-1},L_{j-1})+W^2_{2^j}f(x,y)$$
$$*(L_{j-1},K_{j-1})+S_{2^j}f(x,y)*(\tilde{H}_{j-1},\tilde{H}_{j-1}) \qquad (4)$$

where K and L are the high-pass filters and $\tilde{H}$ is the conjugate filter of H.

A. PWLS Restoration of Low-Dose CT Sinogram

The noise in low-dose CT log-transformed sinogram can be modeled as signal-dependent Gaussian noise, and the variance of noise can be determined by an exponential formula [3, 6]:

$$\sigma^2_i = \alpha_i \times \exp(\ p_i\ /\eta\ ) \qquad (5)$$

where p_i is the mean and σ^2_i is the variance of the projection data at detector i. η and α_i are object-independent parameters and determined by the system or manufacture configuration. Based on the noise properties, a PWLS cost function [12] can be constructed in the sinogram space as:

$$\Phi(p) = (\hat{y}-\hat{p})'\Sigma^{-1}(\hat{y}-\hat{p})+\beta R(p) \qquad (6)$$

The first term in equation (6) is a weighted least-squares (WLS) measure, where ' denotes the transpose operator, $\hat{p}$ is the vector of ideal projection $\{p_i\}$ to be estimated, and vector $\hat{y}$ is the system-calibrated measured projection data (after logarithm transform). Matrix Σ is a diagonal matrix with the ith element of σ^2_i. The second term in equation (6) is a smoothness penalty or *a prior* constraint, where β is the smoothing parameter which controls the degree of agreement between the estimated and the measured data. In this paper, a quadratic smoothness penalty is used [12]:

$$R(p)=p'Rp=\sum_i\sum_{k\in N_i}w_{ik}(p_i-p_k)^2 \qquad (7)$$

where N_i indicates the set of nearest neighbors of the ith pixels in the 2D sinogram and w_{ik} reflects the relative contributions of the nearest neighbors.

The weight in the WLS term of equation (6) plays the role of controlling the contribution of different measured data, where less reliable data contribute less in the PWLS cost function. In this study, the variance of each measured datum is chosen as its weight. By this choice, the PWLS cost function is equivalent to the penalized maximum likelihood (pML) or maximum *a posteriori* probability (MAP) criterion for independent Gaussian distributed noise.

Minimization of the presented PWLS cost function can be performed efficiently by the iterative Gauss-Seidel (GS) updating strategy [4]. The iterative formula for the solution of minimizing equation (6) is given by:

$$p_i^{(n+1)} = \frac{y_i+\beta\sigma^2_i(\sum_{k\in N^1_i}w_{ik}p_k^{(n+1)}+\sum_{k\in N^2_i}w_{ik}p_k^{(n)})}{1+\beta\sigma^2_i\sum_{k\in N_i}w_{ik}} \qquad (8)$$

where index n denotes the iterative number, N^1_i denotes the left and upper nearest neighbors of pixel i, and N^2_i denotes the right and lower neighbors of pixel i.

B. Multiscale PWLS Method

After wavelet transform, noise is contaminated in the wavelet coefficients, especially is dominated in those coefficients at the lowest scale. At the same time, the signal is dominant in the coarsest approximation $S_{2^J}f(x,y)$ of the original image. Based on these observations, we propose to apply PWLS criterion for restoration or de-noising of the wavelet coefficients without modifying the signal-dominant $S_{2^J}f(x,y)$. This multiscale PWLS approach could potentially improve the performance of single-scale PWLS means as described in Section II.B.

As reported in [3, 6, 13], the noise in low-dose CT log-transformed calibrated sinogram can be modeled as Gaussian distribution and the variance of the noise is signal-dependent. It can be shown that the sum of two Gaussian random variables is still a Gaussian variable with its variance being the sum of the variance of the two Gaussian variables. Based on these properties of Gaussian variables and the wavelet transform equations (1) and (2), the noise in wavelet coefficients still follows the Gaussian distribution and the variance of the noise can be calculated as:

$$VW^1_{2^{j+1}}f(x,y)=VS_{2^j}f(x,y)*(G^2_j,D) \qquad (9)$$
$$VW^2_{2^{j+1}}f(x,y)=VS_{2^j}f(x,y)*(D,G^2_j) \qquad (10)$$
$$VS_{2^{j+1}}f(x,y)=VS_{2^j}f(x,y)*(H^2_j,H^2_j) \qquad (11)$$

where $VW^1_{2^j}f(x,y)$, $VW^2_{2^j}f(x,y)$ and $VS_{2^j}f(x,y)$ denote the variance of $W^1_{2^j}f(x,y)$, $W^2_{2^j}f(x,y)$ and $S_{2^j}f(x,y)$. The filter coefficients of G^2_j and H^2_j equal to the square of the filter coefficients in G_j and H_j correspondingly. $VS_{2^0}f(x,y)$ denotes the variance of the initial projection data, and its value is calculated from equation (5). Since the noise in wavelet coefficients still follows the Gaussian distribution, we are able to construct the corresponding PWLS cost function (6) for wavelet coefficients at each resolution scale. In order to consider different signal-to-noise ratios (SNRs) in the wavelet coefficients at different scales, the penalty parameter becomes $\beta/2^j$ at scale j. The optimal wavelet coefficients are then estimated by minimizing the PWLS cost function using the iterative GS updating strategy.

Implementation of the multiscale PWLS algorithm is summarized as following:

1) Calculate the variance image of the original CT sinogram $VS_{2^0}f(x,y)$ according to equation (5).

2) Decompose the sinogram to $\{S_{2^J}f(x,y)$, $(W^1_{2^j}f(x,y))_{1\le j\le J}$, $(W^2_{2^j}f(x,y))_{1\le j\le J}\}$ according to equations (1)-(3), where J is set to 3 in this paper.

3) Calculate the variance of wavelet coefficients according to equations (9)-(11).

4) Restore the wavelet coefficients at each scale by the PWLS criterion via iterative GS update of (8).

5) Compute the de-noised sinogram by inverse wavelet transform on the processed wavelet coefficients.

6) Reconstruct the low-dose CT image from the de-noised sinogram by FBP.

III. RESULTS

A. Experimental Results

To show the effectiveness of the proposed multiscale PWLS method, a 10 mA low-dose CT noisy sinogram was used which was acquired from an anthropomorphic shoulder phantom using a GE multi-slice spiral CT scanner with fan-beam curved detector arrays. The number of bins per view is 888 with 984 views evenly spanned on a circular orbit of 360°. The detector arrays are on an arc concentric to the x-ray source with a distance of 949 mm. The distance from the rotation center to the curved detector band is 408.075 mm. The detector cell spacing is 1.0239 mm.
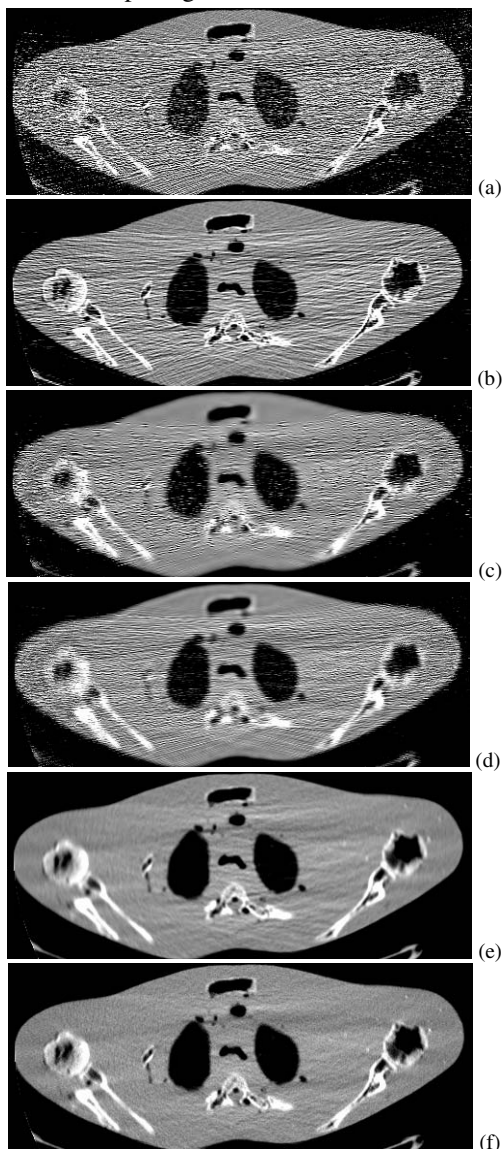

Fig. 1: The CT images from a 10 mA shoulder phantom data: (a) FBP from the sinogram without noise reduction, (b) FBP with Hanning filter at 80% Nyquist cutoff frequency; (c) de-noised result from image (a) by soft-threshold method with db4 wavelets; (d) FBP from de-noised sinogram by soft-threshold method with db4 wavelets; (e) from the single-scale PWLS smoothed sinogram with penalty parameter $\beta = 1 \times 10^{-8}$; and (f) from the multiscale PWLS smoothed sinogram with penalty parameter $\beta = 2 \times 10^{-7}$. The display window is [200, 600].

Fig. 1(a) shows the reconstructed image from the original

sinogram by FBP with Ramp filter at 100% Nyquist frequency. For comparison purpose, reconstructed images by FBP with a spatially-invariant low-pass Hanning filter with cutoff at 80% Nyquist frequency is shown in Fig. 1(b). Figure 1(c) shows the de-noised image of Figure 1(a) using soft-threshold method with db4 wavelets. Figure 1(d) shows the FBP reconstruction from the de-noised sinogram by soft-threshold method with db4 wavelets. Severe noise-induced streak artifacts can be observed in the FBP reconstructed image (a). The Hanning filter and threshold-based wavelet denoising algorithm can not remove the noise and artifacts effectively. Standard FBP (with Ramp at the Nyquist frequency cutoff) reconstructed image from the direct PWLS approach is shown in Fig. 1(e) and from the wavelet-based PWLS method is shown in Fig. 1(f). Both the FBP reconstructions after the PWLS minimizations removed satisfactorily the noise-induced streak artifacts as shown. Manipulating the Hanning filter cutoff frequency or the wavelet threshold in a conventional FBP reconstruction could not reach a comparable noise-resolution tradeoff as that of the two PWLS approaches. In contrary, excellent noise reduction with satisfactory resolution preservation by the two PWLS sinogram-smoothing methods was observed. The performance of the multiscale PWLS seems slightly better than the single-scale PWLS. To further quantitatively evaluate these two PWLS approaches, we performed noise-resolution tradeoff studies as described in the following section.

B. Noise-Resolution Tradeoff Measure on Multiscale and Single-Scale PWLS Approaches

The noise-resolution tradeoffs of the multiscale PWLS method and the single-scale PWLS approach were computed by computer simulations using an ellipse digital phantom. Two hot disks are assumed to be the bone and they are surrounded by tissue-equivalent materials, see Fig. 2. The detector array and X-ray source configuration are exactly the same as the GE scanner as described before. Noise-free sinogram was computed based on the known densities and intersection lengths of the projection rays with the geometric shapes of the objects in the phantom. Noisy sinograms were generated by adding signal-dependent Gaussian noise according to equation (5), simulating the low-mA CT data acquisition protocol.
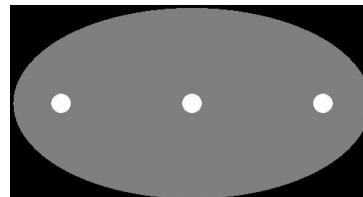

Fig.2. Phantom used for the noise-resolution tradeoff studies.

The reconstructed image resolution was analyzed by the edge spread function (ESF) along the central vertical profile on the left disk and center disk in the reconstructed ellipse-phantom image. The reconstructed image noise was characterized by the standard deviation of a uniform region around the left and the center disks in the reconstructed

ellipse-phantom image. By varying the penalty parameter β for the multiscale PWLS method and the direct PWLS approach, we obtained the noise-resolution tradeoff curve for each approach. The noise-resolution tradeoff curves are shown in Fig. 3. At both the left and the center hot disks, the proposed multiscale PWLS method shows a better performance than the single-scale PWLS approach in all the resolution range. The gain of the multiscale PWLS method over the direct PWLS approach can be explained by the fact that in the proposed multiscale method, the PWLS criterion is only applied on noise-dominant wavelet coefficients of the multi-resolution representation of the original sinogram. There is no modification on the signal-dominant coarsest approximation image $S_{2^J} f(x, y)$. Additionally, the penalty parameter in the presented wavelet-based PWLS method is adaptive to different scales. These considerations lead the proposed method to preserve signal as much as possible and smooth only those noise-dominant components. Indeed, this study concurs with the previous work that the multi-resolution Bayesian tomographic reconstruction outperforms the commonly-used fixed resolution Bayesian methods [14].
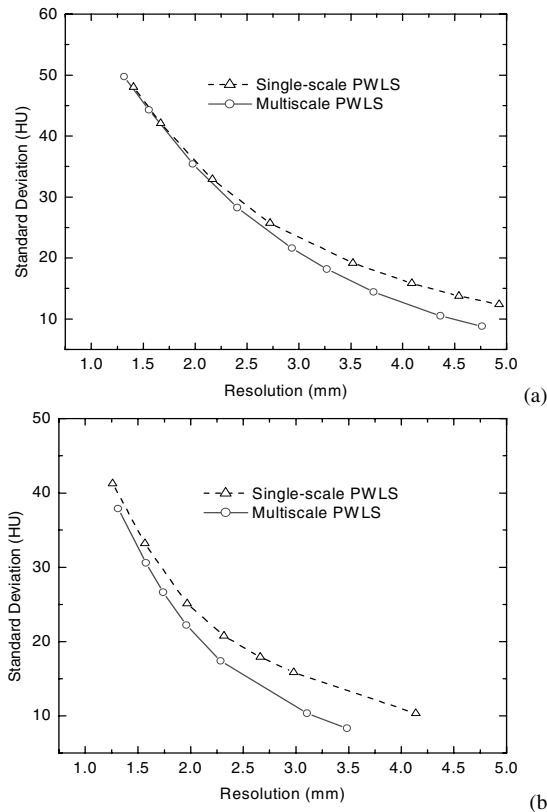

Fig. 3: The noise-resolution tradeoff curves for the presented multiscale PWLS and single-scale PWLS approaches: (a) the left disk and (b) the center disk.

IV. CONCLUSION

With the explicit expression of the relationship between the variance and mean of low-dose CT sinogram, we proposed a novel multiscale PWLS method for restoration of the low-dose CT sinogram. The low-dose CT sinogram was decomposed to different resolution levels using the Mallat-

Zhong's wavelet transform, and a PWLS criterion was applied to restore the wavelet coefficients at each decomposition level. The weights in the PWLS cost function were updated at each decomposition level and the penalty parameter was adaptive to each different scale. The effectiveness of the proposed multiscale PWLS method was demonstrated by an experimental study. The gain by the wavelet-based multiscale PWLS approach was demonstrated by noise-resolution tradeoff measures. This multiscale PWLS method performed better than a single-scale PWLS approach because of its adaptive nature to the signal and noise distributions in the wavelet space. By the use of different thresholds on the wavelet coefficients could not obtain improved results over the PWLS approaches because of the lacking of noise modeling. Due to the same reason, manipulating the frequency cutoff of low-pass noise filters could not generate improved results than the PWLS approaches.

REFERENCES

1. J. Hsieh, "Adaptive streak artifact reduction in computed tomography resulting from excessive X-ray photon noise", *Medical Physics*, vol. 25, pp. 2139-2147, 1998.
2. M. Kachelrie β, O. Watzke, and W.A. Kalender, "Generalized multi-dimensional adaptive filtering for conventional and spiral single-slice, multi-slice, and cone-beam CT", *Medical Physics*, vol. 28, pp. 475-490, 2001.
3. H. Lu, I. Hsiao, X. Li, and Z. Liang, "Noise properties of low-dose CT projections and noise treatment by scale transformations", *Conf. Record IEEE NSS-MIC*, in CD-ROM, 2001.
4. K. Sauer and C. Bouman, "A local update strategy for iterative reconstruction form projections", *IEEE Trans. Signal Processing*, vol. 41, pp. 534-548, 1993.
5. I.A. Elbakri and J.A. Fessler, "Statistical image reconstruction for polyenergetic computed tomography", *IEEE Trans. Medical Imaging*, vol. 21 88-99, 2002.
6. T. Li, X. Li, J. Wang, J. Wen, H. Lu, J. Hsieh, and Z. Liang, "Nonlinear sinogram smoothing for low-dose X-ray CT", *IEEE Trans. Nuclear Science*, vol. 51, pp. 2505-2513, 2004.
7. P.J. La Riviere and D.M. Billmire, "Reduction of noise-induced streak artifacts in X-ray computed tomography through Spline-based penalized-likelihood sinogram smoothing", *IEEE. Trans. Medical Imaging*, vol. 24, pp. 105-111, 2005.
8. D.L. Dohono and I.M. Johnstone, "Ideal spatial adaptation by wavelet shrinkage", *Biometrika*, vol. 81, pp. 425-455, 1994.
9. A. Charnbolle, R.A. De Vore, N.-Y Lee, and B.J. Lucier, "Nonlinear wavelet image processing: variational problems, compression, and noise removal through wavelet shrinkage", *IEEE Trans. Imaging Processing*, vol. 7, pp. 319-335, 1998.
10. J. Zhong, R. Ning, and D. Conover, "Image denoising based on multiscale singularity detection for cone beam CT breast imaging", *IEEE Trans. Medical Imaging*, vol. 23, pp. 696-703, 2004.
11. S. Mallat and S.-F Zhong, "Characterization of signals from multiscale edges", *IEEE Trans. Pattern Analysis and Machine Intelligence*, vol. 14, pp. 710-732, 1992.
12. J.A. Fessler, "Penalized weighted least-squares image reconstruction for positron emission tomography", *IEEE Trans. Medical Imaging*, vol. 13, pp. 290-300, 1994.
13. S. Siltanen, V. Kolehmainen, S. Jarvenpaa, J.P. Kaipio, P. Koistinen, M. Lassas, J. Pirttila, and E. Somersalo, "Statistical inversion for medical X-ray tomography with few radiographs: I. General theory", *Physics in Medicine and Biology*, vol. 48, pp. 1437-1463, 2003.
14. T. Frese, C. A. Bouman, and K. Sauer, "Adaptive wavelet graph model for Bayesian tomographic reconstructions", *IEEE Trans. Image Processing*, vol. 11, pp. 756-770, 2002.